

# **Radio and optical observations of large-scale traveling ionospheric disturbances during a strong geomagnetic storm of 6-8 April 2000**

E. L. Afraimovich<sup>1,\*</sup>, Ya. F. Ashkaliev<sup>2</sup>, V. M. Aushev<sup>2</sup>, A. B. Beletsky<sup>1</sup>,  
L.A. Leonovich<sup>1</sup>, O.S. Lesyuta<sup>1</sup>, A. V. Mikhalev<sup>1</sup>, V. V. Vodyannikov<sup>2</sup>, and A. F.  
Yakovets<sup>2</sup>

\* p. o. box 4026, Irkutsk, 664033, Russia, fax: +7 3952 462557; e-mail: afra@iszf.irk.ru,

<sup>1</sup>Institute of Solar-Terrestrial Physics SD RAS

<sup>2</sup>Institute of Ionosphere, Almaty, 480020, Kazakhstan

Manuscript submitted to

**Journal of Atmospheric and Solar-Terrestrial Physics**

Manuscript version from 3 December 2000

**Offset requests to:**

E. L. Afraimovich

Institute of Solar-Terrestrial Physics SD RAS

Irkutsk, Russia

**Send proofs to:**

E. L. Afraimovich

Institute of Solar-Terrestrial Physics SD RAS

Irkutsk, Russia

## Abstract

Basic properties of the mid-latitude large-scale traveling ionospheric disturbances (LS TIDs) during the maximum phase of a strong magnetic storm of 6-8 April 2000 are shown. Total electron content (TEC) variations were studied by using data from GPS receivers located in Russia and Central Asia. The nightglow response to this storm at mesopause and termospheric altitudes was also measured by optical instruments FENIX located at the observatory of the Institute of Solar-Terrestrial Physics, ( $51.9^{\circ}$  N,  $103.0^{\circ}$  E) and MORTI located at the observatory of the Institute of Ionosphere ( $43.2^{\circ}$  N,  $77.0^{\circ}$  E). Observations of the O (557.7 nm, 630.0 nm, 360-410 nm, and 720-830 nm) emissions originating from atmospheric layers centered at altitudes of 90 km, 97 km, and 250 km were carried out at Irkutsk and of the  $O_2$  (866.5 nm) emission originating from an atmospheric layer centered at altitude of 95 km was carried out at Almaty. Variations of the  $f_0F2$  and virtual altitude of the F2 layer were measured at Almaty as well. An analysis of data was performed for the time interval 17.00-21.00 UT comprising a maximum of the  $D_{st}$  derivative. Results have shown that the storm-induced solitary large-scale wave with duration of 1 hour and with the front width of 5000 km moved equatorward with the velocity of  $200\ ms^{-1}$  to a distance of no less than 1000 km. The TEC disturbance, basically displaying an electron content depression in the maximum of the F2 region, reveals a good correlation with growing nightglow emission, the temporal shift between the TEC and emission variation maxima being different for different altitudes.

---

*Correspondence to:* E. L. Afraimovich

## 1 Introduction

In the course of strong geomagnetic storms, significant changes in main structural elements of the magnetosphere and ionosphere occur. Geophysical manifestations of extremely strong magnetic storms are of particular interest because these storms take place relatively rarely (no more than 4 events during an 11-year solar cycle), and therefore the representative statistics of the whole complex of interactive processes in the "magnetosphere- ionosphere" system is lacking.

We have now reached a new quality level in studying these phenomena because a large number of ionospheric and magnetospheric parameters are continuously monitored by various ground-based and space facilities. A new era in the remote ionospheric monitoring was opened up with the advent of the Global Positioning System (GPS) now comprising more than 800 world-wide two-frequency GPS receivers whose data are available through the INTERNET.

Large-scale traveling ionospheric disturbances (LS TIDs) with a period of 1-2 hours and a wavelength of 1000-2000 km constitute the most significant mid-latitude consequence of magnetic storms. Many papers including review papers (HUNSUCKER, 1982; HOCKE AND SCHLEGEL, 1996) have been published. LS TIDs are considered to be a manifestation of internal atmospheric gravity waves (AGWs) excited by sources in the polar regions of the northern and southern hemispheres. Thus, the study of LS TIDs provides important information on auroral processes under quiet and disturbed geomagnetic conditions.

AFRAIMOVICH et al. (2000) were the first to develop a technique for determining the LS TIDs parameters based on calculations of spatial and temporal gradients of total electron content (TEC) measured by three spaced GPS receivers (a GPS array). This technique was employed to determine the LS TIDs parameters in the course of a strong magnetic storm of 25 September 1998. It was shown that a large-scale solitary wave excited in the auroral region with a duration of about 1 hour and the front width of 3700 km, at least, traveled equatorward to a distance no less than 2000-3000 km with the average velocity of about 300 m/sec.

Another interesting consequence of strong magnetic storms is low-latitude auroras. The global response to the magnetic storm of the year 1989 was studied by YEH ET AL. (1994). Low-latitude auroras were observed in the northern and southern hemispheres. A long-term electron density depression in the mid-latitude ionosphere is the most pronounced effect of the a storm. During the maximum phase of the storm, the zone of disturbances extended to geomagnetic latitudes of less than 10° causing a temporal depression of the equatorial anomaly.

There appeared many papers on the behavior of nightglow emissions of the upper atmosphere

during geomagnetic disturbances (CHAPMAN, 1957; ISHIMOTO ET AL, 1986; TINSLEY, 1979; TORR, 1984). Several peculiarities in spectra of upper atmosphere emissions at the middle and low latitudes during strong geomagnetic perturbations allow them to be classified as "mid- and low-latitude auroras" (RASSOUL ET AL., 1993) distinguishing from the "common" aurora at polar latitudes. The differences between auroras include the appearance of the  $N_2^+$  emission in bands of the first negative system of mid-latitude spectra, a significant increase of the atomic oxygen (630.0 nm) emission, and the predominance of emissions of atomic ion lines above these of molecular bands.

RASSOUL ET AL. (1993) classified several types of low-latitude auroras in relation to the type of bombarding particles (electrons, ions, neutral particles), dominating emissions, localization, and typical temporal scales. Many observations revealed several types of simultaneously existing auroras caused by the bombardment of fast electrons and mixture heavy particles. At mid-latitudes during moderate geomagnetic perturbations, 630 nm emission variations with periods ranging from 0.5 to 2 hours were recorded (MISSAWA ET AL., 1984; SAHAL ET AL, 1988). Mid-latitude auroras occurring in the course of very strong magnetic storms ( $K_p \geq 8-9$ ,  $D_{st} \geq 300$  nT) are of the particular interest because the number of observations with optical instruments was limited.

Although mid-latitude ionospheric storms have been studied during several decades, there is no complete explanation of their effects because of the small number of sounding facilities and their low spatial and temporal resolutions of an ionosonde, a incoherent scatter radar and optical devices. Moreover, in contrast to polar latitudes, a small number of observations were carried out at mid-latitudes simultaneously by radio and optical techniques which supplement each other because they allow their shortcomings to be compensated and the reliability of interpretation of phenomena to be increased.

The objective of this paper is to study the response of the mid-latitude ionosphere to the strong magnetic storm of 6-8 April 2000 by using data of simultaneous radio and optical observations in Russia and Central Asia, main attention being paid to LS TIDs with a characteristic temporal period on the order of 1 hour. Small-scale disturbance, whose increase in intensity is related to the shift of the auroral region toward mid-latitudes, will be the objective of a next study.

Section 2 gives a description of the state of the geomagnetic field on 6-8 April 2000, and the scheme of the experiment. The features of LS TIDs obtained on the basis of TEC and optical and ionosonde data are described in Sections 3 and 4. Section 5 is devoted to the discussion of the results.

## 2 DESCRIPTION OF THE STATE OF THE GEOMAGNETIC FIELD ON 6-8 APRIL 2000, AND SCHEME OF THE EXPERIMENT

Fig. 1 shows the K-index (a), the  $D_{st}$ -variations of the geomagnetic field, and the variations of the H-component of the geomagnetic field at Almaty (c) and Irkutsk (f) in the course of the strong magnetic storm of 6-8 April 2000. This storm was characterized by a pronounced sudden commencement (SSC) that started at 1642 UT. At the maximum of the storm, the K-index achieved the value 8, and a K-index diurnal sum of 48 was observed. At 1600 UT on 6 April, the  $D_{st}$  amplitude increased fast to 0, but after that it began to decrease, and at 2400 UT it reached the value -319 nT. After that, the recovery phase continued into 8 April. In Fig. 1, the dashed vertical lines show SSC and  $t_{min}=20.00$  UT corresponding to the maximum value of the time derivative of  $D_{st}$  ( $dD_{st}/dt$ ).

Fig. 2 shows the scheme of the experiment in the geographical system of coordinates. The positions of the GPS receivers are denoted by heavy dots, and their names are given. On the upper scale, the values of the local time (LT) for a certain longitudinal interval corresponding to the relative time of the arrival of the LS TID at middle latitudes at 19.00 UT are plotted (Section 3). Diamonds and slant letters show the positions of optical instruments MORTI (near Almaty and station SELE) and FENIX (near Irkutsk and station IRKT). Data of an Almaty standard ionosonde were also used in this paper.

GPS receivers are distributed all over the world with a different density, and the region considered in this paper comprises only 11 stations whose coordinates are listed in Table 1. Parameters of LS TIDs are considered to have been determined with a proper reliability when the distances between GPS receivers exceed the wavelength of TIDs (about 1000 km). The array of GPS receivers used in the experiment satisfied this requirement.

## 3 PARAMETERS OF LS TIDS MEASURED BY GPS RECEIVERS AND THE ALMATY IONOSONDE

The GPS technique makes it possible to determine the parameters of TIDs from the phase variations at two carrier frequencies measured at spaced sites. Methods of calculating the relative TEC variations from measurements of the ionosphere-induced change in the phase path of GPS signals were described in detail in several papers (HOFMANN-WELLENHOF ET AL., 1992; AFRAIMOVICH ET AL., 1998, 2000). Here we reproduce the resulting expression for phase

measurements:

$$I_o = \frac{1}{40.308} \frac{f_1^2 f_2^2}{f_1^2 - f_2^2} [(L_1 \lambda_1 - L_2 \lambda_2) + const + nL], \quad (1)$$

where  $L_1 \lambda_1$  and  $L_2 \lambda_2$  are additional paths of the radio signal caused by the phase delay in the ionosphere, (m);  $L_1$  and  $L_2$  represent the number of phase rotations at the frequencies  $f_1$  and  $f_2$ ;  $\lambda_1$  and  $\lambda_2$  stand for the corresponding wavelengths, (m); *const* is the unknown initial phase ambiguity, (m); and  $nL$  are errors in determining the phase path, (m).

For this type of measurements with the sampling rate of 30 seconds, the error of TEC measurements does not exceed  $10^{14} \text{ m}^{-2}$ , the initial value of TEC being unknown (HOFMANN-WELLENHOF et al., 1992). This makes it possible to detect irregularities and waves in the ionosphere over a wide band of amplitudes (up to  $10^{-4}$  of the diurnal TEC variation) and periods (from 24 hours to 5 min). The TEC unit (TECU), which is equal to  $10^{16} \text{ m}^{-2}$  and commonly, accepted in the art, will be used in the following.

Initial data to calculate the parameters of LS TIDs were time-series of TEC at certain sites with corresponding time-series of the angle of elevation  $\Theta(t)$  and azimuth  $\alpha(t)$  for the satellite-receiver line calculated by using software CONVTEC which was able to interpret GPS RINEX-files. Continuous time-series of  $I(t)$  measurements with a duration no less than 3 hours were chosen for determining the LS TIDs parameters.

To exclude trends caused by regular changes in ionospheric density and satellite motion, an hour running average was subtracted from the TEC time-series.  $\Theta(t)$  and  $\alpha(t)$  were employed to calculate coordinates of subionospheric points. To convert the variations of slant TEC to that of vertical TEC, the a well-known technique (KLOBUCHAR, 1986)

$$I = I_o \times \cos \left[ \arcsin \left( \frac{R_z}{R_z + h_{max}} \cos \theta \right) \right], \quad (2)$$

was used, where  $R_z$  is the Earth's radius, and  $h_{max} = 300 \text{ km}$  is the altitude of subionospheric points (near the F2 layer maximum).

### 3.1 Parameters of large-scale traveling ionospheric disturbances determined from GPS data

Fig. 3 and Fig. 4 show the initial  $I(t)$  and detrended time-series  $dI(t)$ . For the YAKZ site, only data from the PRN30 satellite for the interval 17.00 - 20.00 UT were available for technical reasons.

Almost all GPS records show a gradual decrease of  $I(t)$  till a certain time ( $t_{min}$ ) corresponding to minima (designated by diamonds in Fig. 3 and 4) in TEC variations,  $t_{min}$  depending on the latitude of the GPS site. Large fast variations of TEC occur for some sites after  $t_{min}$  has elapsed.

Satellite PRN25 was chosen for all GPS sites analyzed (except YAKZ) because its minimum elevation angle  $\Theta(t)$  exceeded  $45^\circ$  for every station during 19.00 - 21.00 UT. Thus, the error of converting the slanting TEC to vertical one caused by the difference between the actual and spherically-symmetric spatial TEC distributions was minimized.

In Fig. 2, the solid lines show trajectories of motion of subionospheric points for satellite PRN25 (PRN30 for YAKZ) at the altitude of 400 km. Crosses at the trajectories indicate the positions of subionospheric points at  $t_{min}$  corresponding to minimum TEC (Fig. 3, 4). Near crosses one can find the value of  $t_{min}$  expressed in terms of decimal parts of an hour. For the subionospheric point of every GPS station, the values of  $t_{min}$  and amplitudes ( $A_{min}$ ) expressed in TECU are listed in Table 1. As is seen from Fig. 2, a minimum  $dI$  was first recorded for the subionospheric point of station YAKZ at  $57^\circ$  N latitude (thin line in Fig. 3c), and, after that, almost simultaneously it was recorded near  $53^\circ$  N latitude at stations ZWEN, ARTU, KSTU (Fig. 3 a, d; b, e; c, f respectively) which are extended along the same parallel over the longitudinal difference of  $47^\circ$ . Clearly, the ionospheric disturbance had a wave front with its length exceeding 5000 km. Forty minutes later this disturbance was recorded at the subionospheric point for station IRKT at  $51.5^\circ$  N latitude (Fig. 4a, d). Two hours later a similar disturbance  $dI(t)$  was recorded at a chain of stations TRAB, SELE (Fig. 4 b, e), KITS, KUMT and URUM (Fig. 4 c, f) at  $40^\circ$  -  $45^\circ$  N latitudes.

By using Table 1 and Fig. 3 and 4, one can study the evolution of the disturbance as it travels equatorward. The amplitude ( $A_{min}$ ) of the disturbance  $dI(t)$  decreases from 5 TECU at the northern chain of stations to 1 TECU at the southern chain. Moreover, large fast variations  $dI(t)$  typical of the high-latitude ionosphere were recorded after passing a minimum  $dI(t)$  at the northern chain of stations. The same result was obtained by AFRAIMOVICH ET AL. (2000). These variations are noticeably less at the southern chain of stations.

These features of the  $dI(t)$  variations seem to be accounted for the fact that at about 19.00 UT satellite-receiver lines for the northern chain of stations (Fig. 2) crossed the southern boundary of the auroral zone moving southward. If the front of the disturbance has traveled with a constant velocity, then a delay on the order of 2 hours between the times of the rise of the disturbances at the northern and southern chains of stations corresponds to the southward velocity of about 200 m/sec. However, by using the technique of AFRAIMOVICH ET AL. (2000), one can obtain the velocity of about 500 m/sec, and the wave vector directed southeastward. By means of a chain

of ionosondes, MAEDA AND HANNA (1980) and Whalen (1987) obtained similar results. The extension of the disturbance front on the order of 5000 km obtained in this study is consistent with results reported by WHALEN (1987), HAJKOWICZ, AND HUNSUCKER (1987).

So, in the main phase of the strong magnetic storm, a significant descent on the order of 15-20 TECU was observed at the northern chain of GPS sites, including ZWEN, ARTU, KSTU and YAKZ. HUNSUCKER (1982) and BALHAZOR AND MOFFETT (1999) showed that a large area of the polar atmosphere leaving abruptly the state of equilibrium must become the source of LS TIDs traveling equatorward. It is necessary to point out that this period of time was characterized by a maximum time derivative  $D_{st}$  (Fig. 1c) which is consistent with the conclusion of HO ET AL. (1998).

### 3.2 Variations of the critical frequency and virtual altitude of the F2 layer over Almaty

Fig. 1d shows the variations of the critical frequency of the F2 layer ( $f_0F2$ ) (large dots). The solid line represents the  $f_0F2$  current median defined from three- month data (WRENN ET AL., 1987). The day before the magnetic storm was magnetically quiet, and  $f_0F2(t)$  was close to its median values. The main phase of the magnetic storm occurred at local night at Almaty. A decrease of  $f_0F2$  relative to the median, reflecting a depression of the electron content in the F2 layer maximum, began soon after the beginning of the storm and a maximum difference between the current  $f_0F2$  and median values took place at the period of a maximum time derivative  $dD_{st}/dt$ . The growth of  $f_0F2$  after the solar ionizing agent appeared is delayed with respect to the median by two hours. Unfortunately, during 7 hours after 02.00 UT the ionosonde did not operate for technical reasons; therefore, the time at which  $f_0F2$  approached median values was uncertain.

Variations of the virtual altitudes  $h'F$  are plotted in Fig. 1e with large dots. The solid line shows the behavior of the  $h'F$  current median. It is seen from Fig. 1e that an abrupt increase of  $h'F$  with respect to median values began simultaneously with the decrease of  $f_0F2$ . The approach to the median values occurred at 01.00 UT. At that time  $f_0F2$  was equal to 6.0 MHz, and the median value was 11 MHz. The large decrease of  $f_0F2$  in the course of the main phase of the magnetic storm is consistent with the large negative disturbance of TEC recorded by GPS stations (Fig. 4).

Thus, this magnetic storm was accompanied by a very large decrease of the electron content in the maximum of the F2 layer, and by a significant increase of its virtual altitude.

## 4 OPTICAL OBSERVATIONS OF NIGHTGLOW EMISSIONS

#### 4.1 Large-scale disturbances of nightglow emissions over Irkutsk

An optical facility FENIX is settled at Geophysical observatory attached to Institute of Solar-Terrestrial physics at 100 km from Irkutsk city ( $51.9^{\circ}$  N,  $103.0^{\circ}$  E ; geomagnetic latitude is  $41.0^{\circ}$  N, L=2). It includes a four-channel zenith photometer and a high sensitive TV-system comprising an image amplifier and a CCD (charge coupled device) array.

Following observations of nightglow emissions were made: the OI (557.7 nm) emission which originates from a layer centered at 97 km and with boundaries at altitudes of 85 km and 115 km, the OI (630.0 nm) emission which originates from a layer centered at 250-270 km and with boundaries at altitudes of 160-300 km, the  $O_2$  (360-410 nm) emission which originates from a layer centered at 97 km, and the OH emission which originates from a layer centered at 85-90 km and with boundaries at altitudes of 75-115 km.

Emission lines of 557.7 and 630 nm were recorded by using narrow band (1-2 nm halfwidth) sweeping interference filters. Records of 360-410 nm and 720-830 emissions were obtained by using broad band absorption filters. The angle of view of instruments was about 4-5. The instruments were absolutely calibrated periodically by using the standard stars and were controlled by using reference lamps in periods between absolute calibrations. The software provided records of the emission rate with an exposure time of 12 sec, but when the emission rate exceeded the predetermined level, a shorter exposure time of 8 ms was used. In the course of the magnetic storm of 6 April 2000, the records were taken only by the four-channel zenith photometer.

Variations of the nightglow emission rate, derived from the zenith photometer observations on 6 April 2000, are plotted in Fig. 5a. The main feature of these variations is a significant increase of the OI (630.0 nm) emission in the second half of the night (Fig. 5a, line 1) by a factor of 20 compared with values observed near midnight and the last geomagnetic quiet night of 5 April 2000 (Fig. 5a, line 3). It can be seen that the OI (630.0 nm) emission grew after 16.00 UT till sunrise when the observations were completed, and periodical variations were superimposed on the gradual growth. The OI (557.7) emission variations (Fig. 5a, line 2) revealed a small disturbance near 17.00 UT coinciding with a similar disturbance in the OI (630.0 nm) emission, and an abrupt rise (35%) coinciding with the first phase of the OI (630.0 nm) emission rate maximum increase.

A gradual increase of  $O_2$  (360-410 nm) emission, not typical of the quiet geomagnetic state (Fig. 5b, line 6 for the previous night of 5 April 2000) (Fig. 5b, line 4) was observed with superimposed irregular short-period variations, to begin at 17.00 UT. The 720-830 nm emission (Fig. 5b, line 5) revealed a gradual decrease from 14.00 till 16.00 UT and ended at 16.00 UT when the

commencement of the geomagnetic storm occurred.

It is of interest to compare these data with variations of TEC measured at the nearest GPS station IRKT. Records of the 630 nm and 577.7 nm emission lines ( $A(t)$ ) and ( $B(t)$ ) filtered out from the initial data (Fig. 5a, lines 1 and 2 respectively) as it was done with TEC  $I(t)$ , are plotted in Fig. 4d. It is seen that there is a good correlation between these variations, and the emission variations are in an opposite phase compared with TEC variations. The possible reasons for this behavior are discussed in part 6.

#### 4.2 Large-scale disturbances observed by the MORTY instrument

The MORTI (Mesopause Rotational Temperature Imager) instrument is installed near Almaty in the mountains at 2800 m above sea level ( $43.05^{\circ}$  N,  $76.97^{\circ}$  E). MORTI provides information for obtaining the rotational temperature and emission rate of the  $O_2$  atmospheric (0-1) nightglow layer centered at 95 km (WIENS ET AL., 1991). The instrument comprises a conical mirror to receive the light from a full circle, a narrow band (0.27 nm halfwidth) interference filter centered at 867.6 nm, an imaging lens to focus the spectrum, and a CCD camera to record the spectrum. The emission rate and temperature observations have the precision of  $\pm 2\%$  and  $\pm 2$  K, respectively, when the exposure time is 5 min.

Variations of the  $O_2$  (867.6 nm) emission on 6 April 2000 are plotted by dots in Fig. 6a, and detrended variations are shown in Fig. 6b. The quadratic trend calculated by the least square technique (Fig. 6a, solid line) was subtracted from the initial record to obtain the detrended variations. It is seen that large variations in the  $O_2$  (867.6 nm) emission were observed even before the time of the arrival of the solitary wave caused by the magnetic storm (this time is known from the GPS data). The period of background variations was about 2 hours, so the solitary wave excited by the magnetic storm can be distinguished because its period was about 1 hour. In order to reduce the effect of two-hour background variations the high pass filter realized by the hour running window was applied to the record in Fig. 6b. Filtered variations of the  $O_2$  (867.6 nm) emission are plotted in Fig. 4e together with variations of TEC  $I(t)$  for the GPS station SELE. It is seen from Fig. 4e that there is a good correlation between the variations from the GPS and MORTI data. By comparing Fig. 4d and Fig. 4e, it becomes evident that the phase delays between the variations of the GPS and MORTI data are different for Irkutsk and Almaty. This difference is explicable by the different altitudes of the nightglow emissions, and the different types of optical instruments.

## 5 DISCUSSION

The parameters of the disturbances considered in this study are affected by various factors. These are the localization and dynamics of the main ionospheric trough (MIT), the plasmasphere and the plasmapause, the zone of precipitating particles (auroral oval), and magnetospheric-ionospheric currents. During periods of great geomagnetic activity, the plasmapause boundary may approach extreme values of L in the range of 1.7-2.5 (KHOROSHEVA, 1987), the position of MIT - about 43° N of invariant latitude (ANNAKULIEV ET AL., 1997), and the auroral oval boundaries - about 48° N corrected geomagnetic latitudes (<http://www.sec.noaa.gov/Aurora/index.html>). For Irkutsk this latitude is equal to 47° N. According to the data from satellite NOAA-15 (<http://sec.noaa.gov/pmap/pmapN.html>) near sunrise of 7 April 2000, the auroral oval boundary (on the level of 0.1  $erg/cm^2s$ ) approached 56 – 58° N geographical latitudes in the longitude sector under consideration. Taking into consideration that the width of MIT is of several degrees, it is possible to consider that, at least, the southern boundary of MIT approached the latitude of 52° N in Eastern Siberia where optical observations were carried out. These facts suggest that in the course of the magnetic storm considered, elements of the subauroral and even auroral ionosphere were observed at latitudes of Irkutsk. This conclusion is supported by some features of optical observations. The signal gain in the spectral band of 360-410 nm after 17.00 UT may be the result of a rise of the  $N_2^+$  (ING) emission with a wavelength of 391.4 nm which is usually observed in auroras after the ionization of  $N_2$  by precipitating electrons or precipitation of energetic atoms or ions (ISHIMOTO et al., 1986; TINSLEY et al., 1984).

Beside the known fact of the increase of the 630.0 nm emission in midlatitudes auroras, there is a maximum in the 630.0 nm emission at about 19.30 UT, which corresponds to a minimum TEC at almost the same place (Fig. 4d). The same behavior of the 630.0 nm emission was observed above Irkutsk in the course of the strong magnetic storm of 24-25 March 1991 (MIKHALEV, 1997). If a minimum in TEC variations is related to the passage of MIT during the increase of the ring current in the start phase of the magnetic storm, then it is possible to conclude that the maximum 630.0 nm emission develops in the region of MIT where stable auroral red (SAR) arcs occur (REES and ROBLE, 1975).

In connection with the issue discussed, the results of LOBZIN AND PAVLOV (1998) on SAR arcs above North America are of certain interest. In the cited paper, it was pointed out that the pale glow in the form of SAR arcs might become the phenomenon of low-latitude aurora during strong magnetic disturbances. During strong magnetic storms ( $D_{st} > -200$  nT) the 630 nm emission

rate from the SAR arcs approaches 2.2 - 4.0 kR. The 630 nm emission rate recorded during the magnetic storm considered above Irkutsk is in this emission range. Identifications of the SAR arcs and midlatitudes lights were carried out at other papers (for example, KHOROSHEVA, 1987).

For the SAR arcs, an increase of populating  $^1D$  neutral oxygen originates from growing electron temperature at altitudes of the F2-layer and outer ionosphere caused by an increase of the heat flow from the plasmasphere where an interchange of energy between the heat plasma and ring current occurs. The different pattern of the change of short-period variations in the nightglow emissions before and after the TEC minimum must be emphasized where the amplitude of these variations after the TEC minimum is sharply increased. Besides, they correlate with short-period variations of TEC (Fig. 3 and Fig. 4 a, d). The rise of the short-period variations appears to be caused by precipitation of energetic particles.

According to BURNS et al. (1991), TEC is directly proportional to the ratio  $O / (O_2 + N_2)$ , therefore when the  $N_2$  increases the local and integral electron contents decrease, and this fact is consistent with results obtained (Fig. 4).

## 6 CONCLUSION

Thus, in the course of the magnetic storm of 6 April 2000, two types of disturbances were observed. The first one has features of a solitary wave with a period of about 1 hour, and was interpreted as an LS TID originating in the polar latitudes. The second one included short-period variations probably related to the particle precipitation. Alternatively, the wave-like disturbance may be interpreted as a motion of structural element projections of the disturbed ionosphere (the plasmapause and MIT) on to the region of midlatitudes during the start stage of the magnetic storm. In this case, during a strong magnetic storm the elements of the subauroral ionosphere were observed at the latitudes of Irkutsk.

An analysis of the data has shown that being originated the auroral disturbance induced LS solitary wave with a period of about 1 hour and the front width no less 5000 km traveled equatorward to a distance no less than 1000 km with the average velocity of about 200 m/s. The TEC disturbance, showing mainly a decrease of the electron content in the vicinity of the F2-layer maximum, correlates with an increase of the emission rate in the optical band, with the temporal shift being different for different ionospheric altitudes.

At Almaty the magnetic storm was followed by an extremely large decrease of the electron content in the F2-layer maximum which caused a decrease of the nighttime critical frequencies by

4-5 MHz. The decrease of the electron content was accompanied by a significant increase of the F2-layer virtual height.

*Acknowledgements.* We are grateful to E.A. Ponomarev and A.V. Tashchilin for their encouraging interest in this study, and for active discussions. This work was done with support of INTAS grant  $N \simeq 99-1186$ , Leading Scientific Schools of Russian Federation grant  $N \simeq 00-15-98509$  and Russian Foundation for Basic Research grant  $N \simeq 99-05-64753$ .

## References

**AFRAIMOVICH, E. L., K. S. PALAMARTCHOUK AND N. P. PEREVALOVA** (1998) GPS radio interferometry of travelling ionospheric disturbances. *J. Atmos. and Sol.-Terr.Phys.*, 60, 1205-1223.

**AFRAIMOVICH, E. L., E. A. KOSOGOROV, L. A. LEONOVICH, K. S. PALAMARTCHOUK, N. P. PEREVALOVA, AND O. M. PIROG** (2000) Determining parameters of large-scale traveling ionospheric disturbances of auroral origin using GPS-arrays. *J. Atmos. and Sol.-Terr.Phys.*, 62, 553-565.

**ANNACULIEV, C. K., V. V. AFONIN, M. G. DEMIDOV, A. T. KARPACHEV** (1997) Empirical formula for the main ionospheric trough during a magnetic storm. *Geomag. i aeron.*, 37, 3, 183-187.

**AUSHEV, V. M., A. I. POGORELTSEV, V. V. VODYANNIKOV, R. H. WIENS AND G. G. SHEPHERD** (2000) Results of the Airglow and Temperature Observations by MORTI at the Almaty Site (43.05° N, 76.97° E). *Phys. Chem. Earth (B)*, 25, 5-6, 409- 415.

**BALTHAZOR, R. L. AND R. J. MOFFETT** (1999) Morphology of large-scale traveling atmospheric disturbances in the polar thermosphere. *J. Geophys. Res.*, 104, A1, 15-24.

**BURNS, A. G. AND T. L. KILLEN, R. G. ROBLE** (1991) A Theoretical Study of Thermospheric Composition Perturbation During an Impulsive Geomagnetic Storm, *J. Geophys. Res.*, 96, No A8, 14,153-14,167, August 1, 1991.

**CHAPMAN, S.** (1957) The aurora in middle and low latitude. *Nature*, 179, 7.

**KHOROSHEVA, O. V.** (1987) On relations auroral forms and low-latitudes red arcs. *Geomag. i aeron.*, 27, 5, 804-811.

**HAJKOWICZ, L. A. AND R. D. HUNSUCKER** (1987) A simultaneous observation of large-scale periodic TIDs in both hemispheres following an onset of auroral disturbances. *Planet. Space Sci.*, 35, 6, 785-791.

**HO, C. M., B. A. IIJIMA, X. P. LINDQWISTER, A. J. MANNUCCI, L. SPARKS, M. J. REYES AND B. D. WILSON** (1998) Ionospheric total electron content perturbations monitored by the GPS global network during two northern hemisphere winter storms. *J. Geophys. Res.*, 103, 26409-26420.

**HOFMANN-WELLENHOF, B., H. LICHTENEGGER AND J. COLLINS** (1992) Global Positioning System: Theory and Practice, Springer-Verlag Wien, New York.

**HOCKE, K. AND K. SCHLEGEL** (1996) A review of atmospheric gravity waves and travelling ionospheric disturbances: 1982-1995. *Ann. Geophys.*, 14, 917-940.

**HUNSUCKER, R. D.** (1982) Atmospheric gravity waves generated in the high-latitude ionosphere. A review. *Rev. Geophys.*, 20, 293-315.

**ISHIMOTO, M., M. R. TORR, P. G. RICHARDS, AND D. G. TORR** (1986) The role of energetic O+ precipitation in a mid-latitude aurora. *J. Geophys. Res.*, 91, 5793.

**KLOBUCHAR, J. A.** (1986) Ionospheric time-delay algorithm for single-frequency GPS users, *Trans. on Aerospace and Electronics System*, 23(3), 325-331.

**LOBZIN V. V., A. B. PAVLOV** (1998) Relationships of nightglow intensity of subauroral arcs with solar

and magnetic activity. *Geomag. i aeron.*, 38, 4, 49-61.

**MAEDA, S. AND S. HANDA** (1980) Transmission of large-scale TIDs in the ionospheric F2-region. *J. Atmos. Terr. Phys.*, 42, 853-859.

**MIKHALEV, A. V.** (1997) Photometric Observation of Midlatitude Auroras over South-East Siberia. 8th Scientific Assembly of IAGA with ICMA and STP Symposia. Uppsala, August 4-15, Abstracts, p.161.

**ISAWA, K., I. TAKEUCHI, I. AOYAMA** (1984) Apparent progression of intensity variations of the oxygen red line. *J. Atmos. Terr. Phys.*, 46, 1, 39-46.

**RASSOUL, H. K., R. P. ROHRBAUGH, B. A. TINSLEY AND D. W. SLATER** (1993) Spectrometric and Photometric Observation of Low-Latitude Aurorae. *J. Geophys. Res.*, 98, A5, 7695-7709.

**REES, M. H., R. G. ROBLE** (1975) Observations and theory of the formation of stable auroral red arcs. *Rev. Geophys. Space Phys.*, 13, 1, 201.

**SAHAL, Y., J. A. BITTENCOURT, H. TAKAHASILI, N. R. TEIXEIRA, J. H. SOBRAL, B. A. TINSLEY, R. P. ROHRBAUGH** (1988) Multispectral optical observations of ionospheric F-region storm effects at low latitude. *Planet. Space Sci.* 36, 4, 371-381.

**TINSLEY, B. A.** (1979) Energetic neutral atom precipitation during magnetice storm: Optical emission, ionization, and energy deposition at low and middle latitudes. *J.Geophys. Res.*, 84, 1855.

**TINSLEY, B. A., R. P. ROHRBAUGH, H. RASSOUL, E. S. BARKER, A. L. COCHRAN, W. D. COCHRAN, B. J. WILLS, D. W. WILLS, D. SLATER** (1984) Spectral characteristics of two types of low latitude aurorae. *Geophys. Res. Lett.*, 11, 6, 572-575.

**TORR, M. R., AND D. G. TORR** (1984) Energetic oxygen in mid-latitude aurora. *J.Geophys. Res.*, 89, 5547.

**WHALEN, J. A.** (1987) Daytime F-layer trough observed on a macroscopic scale. *J. Geophys. Res.*, 92, 2571-2576.

**WIENS, R. H., S. P ZHANG, R. N. PETERSON, G. G. SHEPHERD** (1991) MORTI: A Mesopause Oxygen Rotational Temperature Imager. *Planet. Space Sci.*, 39, 1363-1375.

**WRENN, G. L., A. S. RODGER, H. RISHBETH** (1987) Geomagnetic storm in the Antarctic F-region. *J. Atmos. Terr. Phys.*, 49, 9, 901-913.

**YEH, K. C., S. Y. MA, K. H. LIN AND R. O. CONKRIGHT** (1994) Global ionospheric effects of the October 1989 geomagnetic storm. *J. Geophys. Res.*, 99, A4, pp.6201-6218.

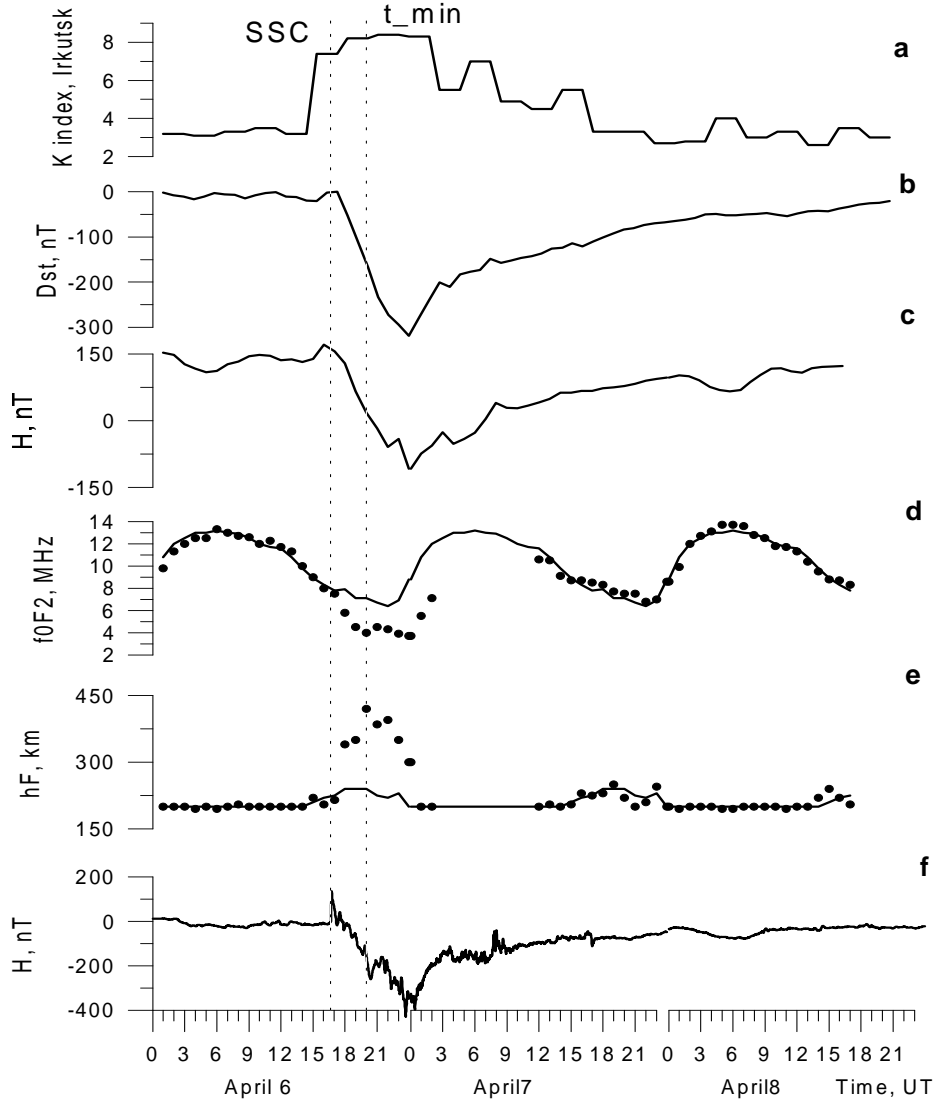


Fig. 1: K-index (**a**),  $D_{st}$ -variations of the geomagnetic field (**b**), variations of the H-component of the geomagnetic field at Almaty (**c**), and Irkutsk (**f**) during the great magnetic storm of 6-8 April, 2000. Variations of the critical frequency  $f_0F2$  (**d**) and virtual height  $h'F$  of the F2-layer (**e**) at Almaty (heavy dots); current median meanings of these parameters are plotted by thin lines. Dashed vertical lines denote moments of SSC and  $t_{min}$ , the interval inside these moments being corresponded the maximum value of  $dD_{st}/dt$ .

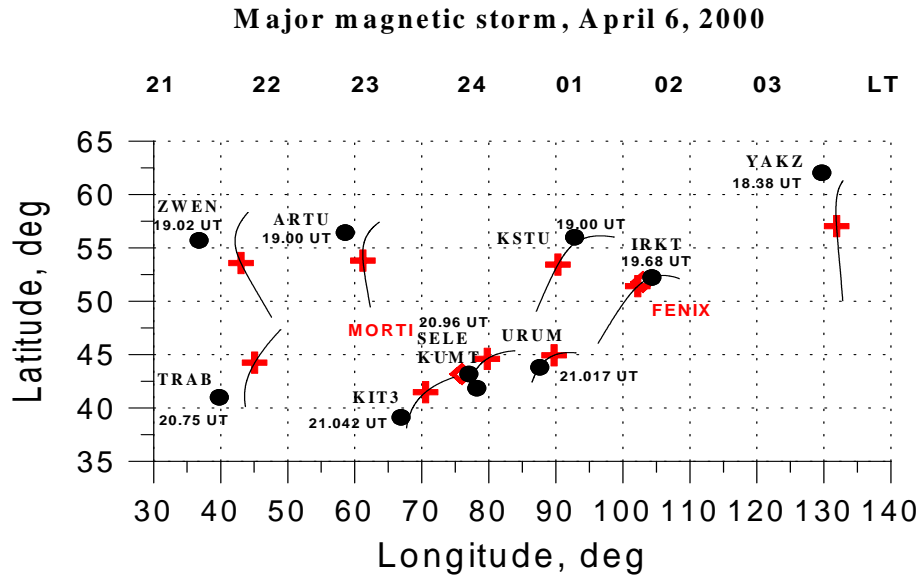


Fig. 1: A scheme of the experiment in the geographical system of coordinates. Positions of GPS receivers are denoted with heavy dots and their names are placed there. Solid lines represent trajectories of subionospheric points motion for the satellite PRN25 at the altitude of 400 km. Crosses at the trajectories denote positions of subionospheric points at moments  $t_{min}$  when minimum TEC occurs (see Fig. 3 and Fig. 4);  $t_{min}$  expressed in decimals of an hour (UT). On the upper scale, values of a local time (LT) for the certain longitude interval corresponding to the relative time of the arrival of the LS TID in middle latitudes at 19.00 UT are plotted (Section 3). Diamonds and slant letters show positions of optical instruments MORTI (near Almaty and station SELE) and FENIX (near Irkutsk and station IRKT).

**Great magnetic storm of April 6, 2000**  
**PRN25**

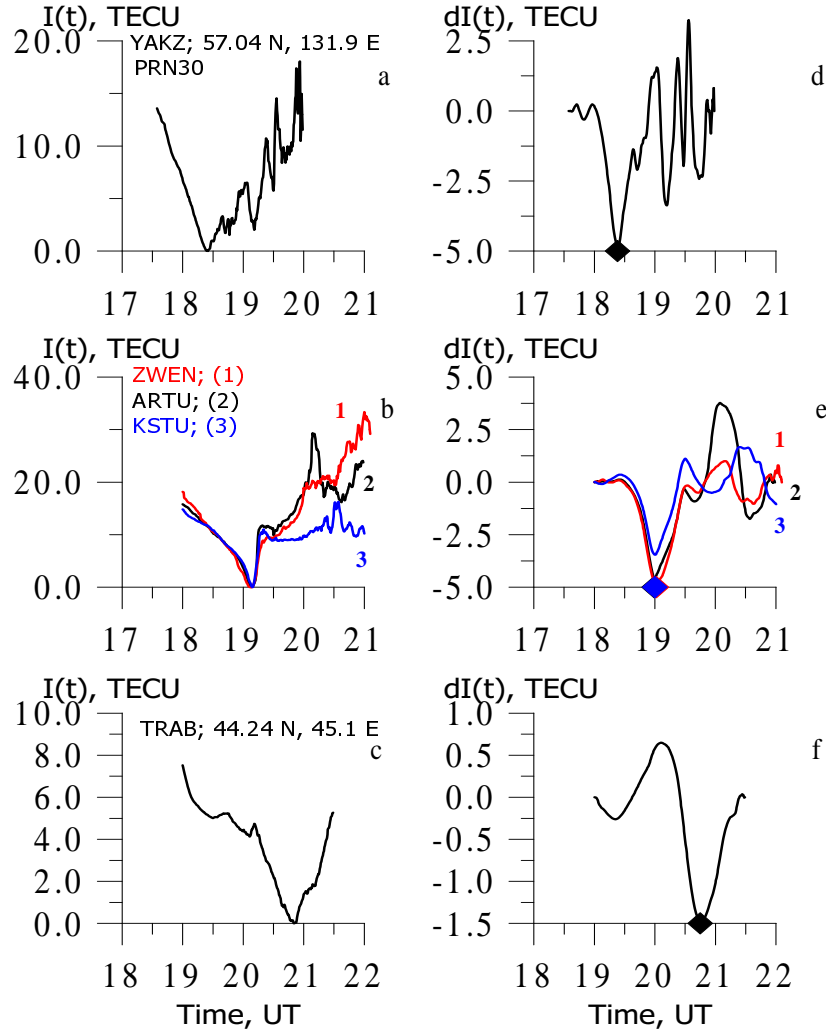


Fig. 1: The initial time-series of slant TEC,  $I(t)$ , at GPS stations ZWEN, ARTU, KSTU for satellite PRN25 on 6 April, 2000 (b) and TRAB (c); and detrended ones,  $dI(t)$ , (e), and (f) . Panels (a) and (b) represent  $I(t)$  and  $dI(t)$  variations at the station YAKZ for satellite PRN30. Geographical coordinates of subionospheric points for every station at  $t_{min}$  are plotted at panels (a), (b), (c). Diamonds at temporal axes denote moments,  $t_{min}$ , of minimum  $dI(t)$ .

### Great magnetic storm of April 6, 2000 PRN25

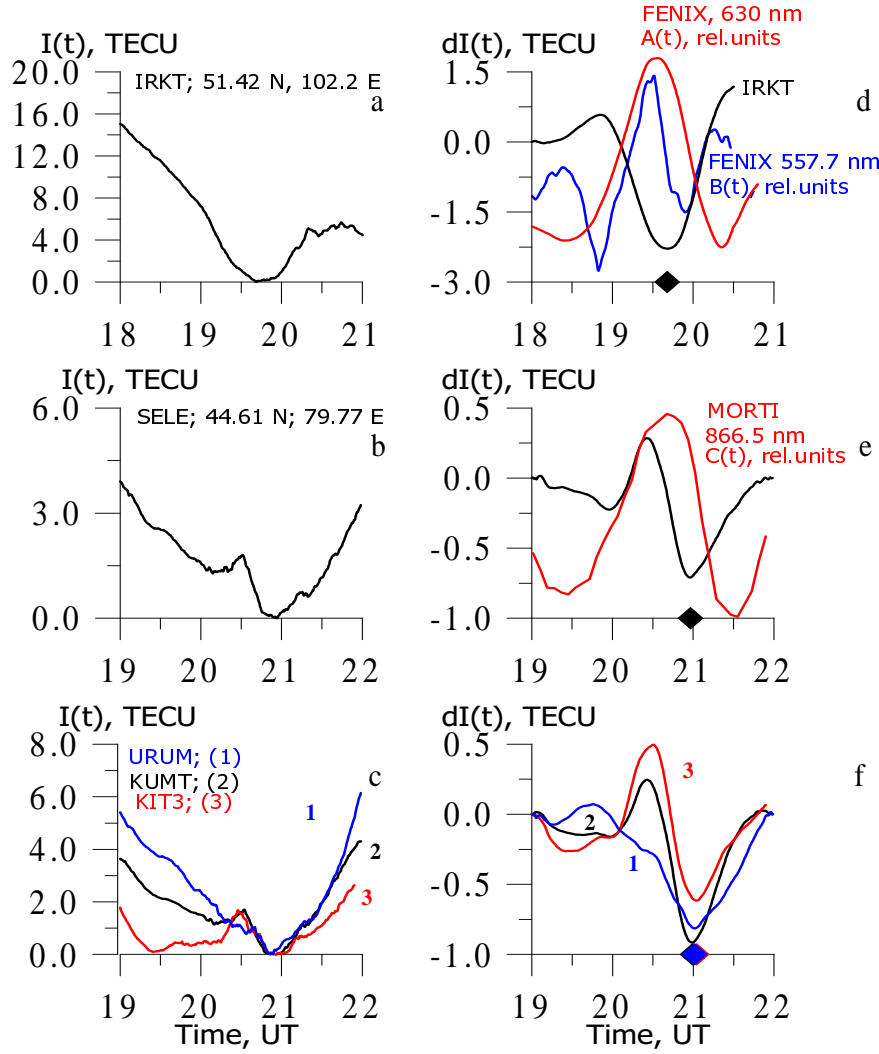


Fig. 1: As in Fig. 3, but for GPS stations IRK (a, d), SELE (b, e), KUMT, KIT3, and URUM (c, f). For comparison, thin lines at the panel (d) show behavior of the 630 nm emission rate ( $A(t)$ ) and the 577.7 nm emission rate ( $B(t)$ ) recorded by the instrument FENIX and filtered from initial data (Fig. 5a, curves 1, 2, respectively), as it was done for TEC data,  $I(t)$ . Behavior of the 866.5 nm emission rate ( $C(t)$ ) recorded by the instrument MORTI and filtered from initial data (Fig. 6b), as it was done for TEC data,  $I(t)$ .

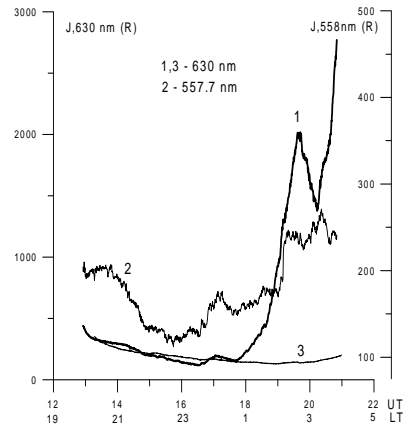
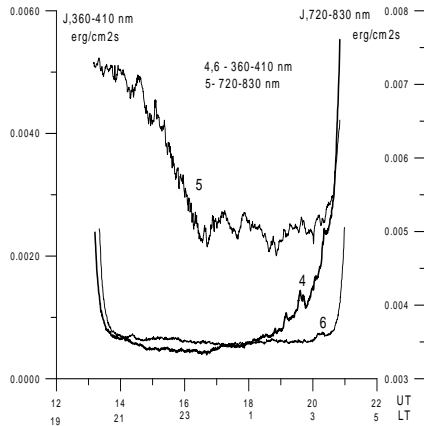
**a****b**

Fig. 1: Variations of the 630 nm and 577.7 nm emission rates (curve 1, 2, respectively) during magnetic storm of 6 April, 2000 in universal (UT) and local (LT) times (a). Variations of the nightglow emissions at spectral band of 360-410 nm (curve 4) and 720-830 nm (curve 5) (b). For comparison, variations of the 630 nm emission rate (curve 3) and emission rate in the band of 360 - 410 nm (curve 6) corresponded to the magnetically quiet night of 5 April, 2000 are plotted. Data were obtained by FENIX instrument.

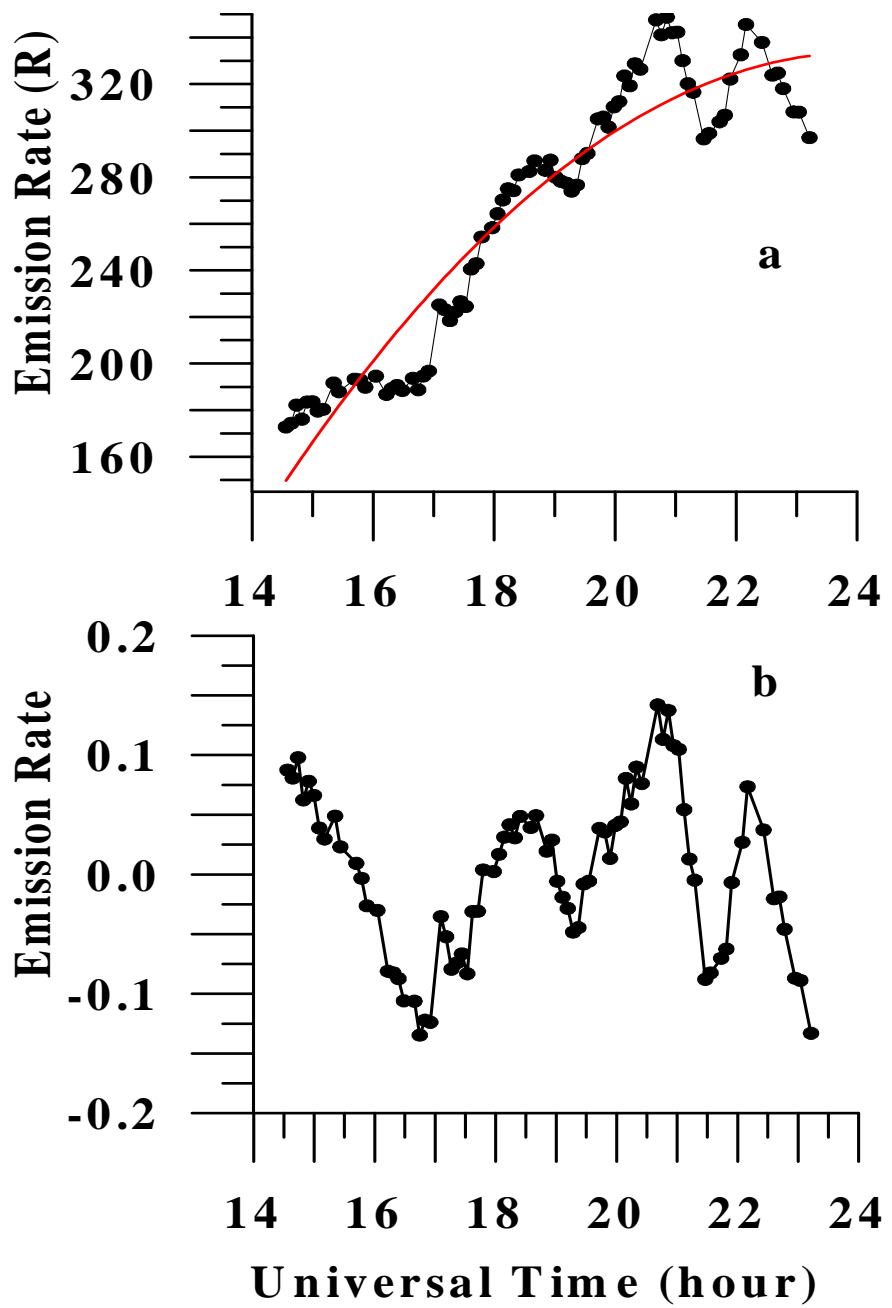


Fig. 1: Initial variations of the 866.5 nm emission rate (a) and detrended ones (b) during the magnetic storm of 6 April, 2000. Data are obtained by MORTI instrument.